

Figure Captions

Chapter 2

Fig. 2-1 Sheet resistance vs. annealing temperature for NiSi(310Å)/Si samples implanted with BF_2^+ at various energies to a dose of $2 \times 10^{15} \text{ cm}^{-2}$. The sample without ion implantation is designated as control sample.

Fig. 2-2 Sheet resistance vs. annealing temperature for NiSi(310Å)/Si samples implanted with BF_2^+ at various energies to a dose of $5 \times 10^{15} \text{ cm}^{-2}$. The sample without ion implantation is designated as control sample.

Fig. 2-3 Sheet resistance vs. annealing temperature for NiSi(310Å)/Si samples implanted with BF_2^+ , B^+ , and F^+ ions. The control sample stands for the NiSi(310 Å)/Si sample without any ion implantation.

Fig. 2-4 SIMS depth profiles of fluorine in NiSi(310Å)/Si samples implanted with BF_2^+ at 35 keV to a dose of 2×10^{15} as well as $5 \times 10^{15} \text{ cm}^{-2}$ followed by 750°C thermal annealing.

Fig. 2-5 Top view SEM micrograph showing the surface morphology of non-implanted NiSi(310Å)/Si control sample annealed at (a) 600, (b) 700 (c) 750, and (d) 800°C for 30 min.

Fig. 2-6 SEM micrographs showing the surface morphology of BF_2^+ (35keV) implanted NiSi (310Å)/Si samples annealed at (a) 700, (b)750, and (c)

800°C for 30 min. The low-dose ($2 \times 10^{15} \text{ cm}^{-2}$) and high-dose ($5 \times 10^{15} \text{ cm}^{-2}$) implanted samples are shown on the left and right columns, respectively.

Fig. 2-7 SEM micrographs showing the surface morphology of Si substrate after removal of NiSi film from the 700 (left) and 750°C (right) annealed NiSi/Si samples: (a) control sample, (b) sample implanted with BF_2^+ at 35keV to a dose of $2 \times 10^{15} \text{ cm}^{-2}$, and (c) sample implanted with BF_2^+ at 35keV to a dose of $5 \times 10^{15} \text{ cm}^{-2}$.

Fig. 2-8 Sheet resistance vs. RTA temperature for NiSi(310Å)/Si samples implanted with BF_2^+ at various energies to a dose of $5 \times 10^{15} \text{ cm}^{-2}$. The sample without ion implantation is designated as control sample.

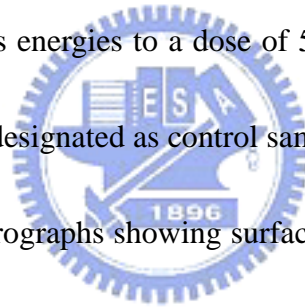


Fig. 2-9 Top view SEM micrographs showing surface morphology of NiSi(310Å)/Si samples annealed with RTA for 30 sec at various temperatures: (a) control sample at 650°C, (b) control sample at 750°C, (c) control sample at 800°C, and (d) BF_2^+ (35keV) implanted sample at 800°C.

Fig. 2-10 Sheet resistance vs. annealing temperature for NiSi(615Å)/Si samples implanted with P^+ (single implantation) and P^+/F^+ (dual implantation) at various implantation conditions. The sample without any ion implantation is designated as control sample.

Fig. 2-11 XRD spectra for sample P2 (implanted with P^+ ions at 50keV to a dose of

$5 \times 10^{15} \text{cm}^{-2}$) annealed at various temperatures. NiSi_2 phase appears after annealing at 750°C .

Fig. 2-12 SIMS depth profile of fluorine in sample P2F5 (dual implantation with P^+/F^+ ions at 50/30 keV to a dose of $5 \times 10^{15}/5 \times 10^{15} \text{cm}^{-2}$) annealed at 750°C .

Fig. 2-13 SEM micrographs showing surface morphology of $\text{NiSi}(615\text{\AA})/\text{Si}$ control sample annealed at (a) 600, (b) 650, (c) 700, and (d) 750°C for 90 min.

Fig. 2-14 SEM micrographs showing surface morphology of ion implanted NiSi/Si samples of (a) P2, (b) P2F2, (c) P2F4, and (d) P2F5 annealed at 750°C for 90 min.

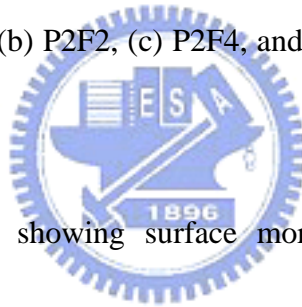


Fig. 2-15 SEM micrographs showing surface morphology of Si substrate after removal of silicide layer from the 750°C -annealed samples of (a) P2, (b) P2F2, (c) P2F4, (d) P2F5, and (e) P1F5.

Chapter 3

Fig. 3-1 Schematic illustration of the Kelvin contact resistance test pattern.

Fig. 3-2 Cross sectional view of the Kelvin contact resistance test pattern of Fig. 3-1 along line 3-4.

Fig. 3-3 Process flow of fabricating the Kelvin structure for $\text{NiSi}/\text{p}^+\text{n}$ contact

resistance measurements.

Fig. 3-4 The as-implanted boron profiles obtained by TRIM simulation for BF_2^+ implantation into a 310-Å-thick NiSi film on Si substrate to a dose of $5 \times 10^{15} \text{ cm}^{-2}$ at various energies.

Fig. 3-5 Forward ideality factor vs. annealing temperature for the NiSi(310Å)/p⁺n junction diodes fabricated with BF_2^+ implantation at various energies to a dose of $5 \times 10^{15} \text{ cm}^{-2}$.

Fig. 3-6 Reverse bias current density vs annealing temperature for the NiSi(310Å)/p⁺n junction diodes fabricated with BF_2^+ implantation at various energies to a dose of (a) $2 \times 10^{15} \text{ cm}^{-2}$ and (b) $5 \times 10^{15} \text{ cm}^{-2}$.

Fig. 3-7 Arrhenius plots of reverse current I_R for the NiSi(310Å)/p⁺n junctions (with an area of $1100 \times 1100 \mu\text{m}^2$) fabricated by BF_2^+ implantation at 20 and 35 keV to a dose of $5 \times 10^{15} \text{ cm}^{-2}$ followed by 650 to 750°C annealing for 30 min. The measurement was conducted at 1V reverse bias.

Fig. 3-8 The J^R vs. P/A plot of the NiSi(310Å)/p⁺n junctions fabricated with BF_2^+ implantation at 20 keV to a dose of $5 \times 10^{15} \text{ cm}^{-2}$ followed by annealing at 550 to 750°C.

Fig. 3-9 Typical I-V characteristic for the NiSi(310Å)/p⁺n junction fabricated with BF_2^+ implantation at 35keV to a dose of $5 \times 10^{15} \text{ cm}^{-2}$ followed by a 30 min

thermal annealing at 700°C.

Fig. 3-10 Ideality factor vs. RTA temperature for the NiSi(310Å)/p⁺n junction diodes fabricated with BF₂⁺ implantation at various energies to a dose of 5×10¹⁵cm⁻².

Fig. 3-11 Reverse bias current density vs. RTA temperature for the NiSi(310Å)/p⁺n junction diodes fabricated with BF₂⁺ implantation at various energies to a dose of 5×10¹⁵cm⁻².

Fig. 3-12 Typical I-V characteristic for the NiSi(310Å)/p⁺n junction (with an area of 580×580μm²) fabricated with BF₂⁺ implantation at 35keV to a dose of 5×10¹⁵cm⁻² followed by RTA at 650°C.

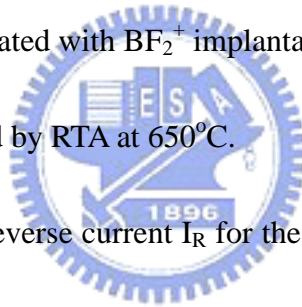


Fig. 3-13 Arrhenius plots of reverse current I_R for the NiSi(310Å)/p⁺n junctions (with an area of 580×580μm²) fabricated by BF₂⁺ implantation at 20 and 35 keV to a dose of 5×10¹⁵cm⁻² followed by RTA at 650 to 750°C. The measurement was conducted at 1V reverse bias.

Fig. 3-14 Arrhenius plots of reverse current I_R for the NiSi(310Å)/p⁺n junctions of three different junction areas fabricated with BF₂⁺ implantation at 35 keV to a dose of 5×10¹⁵cm⁻² followed by RTA at 750°C. The measurement was conducted at 1V reverse bias.

Fig. 3-15 The J_R' vs. P/A plot for the NiSi(310Å)/p⁺n junctions fabricated with BF₂⁺

implantation at 35 keV to a dose of $5 \times 10^{15} \text{ cm}^{-2}$ followed by RTA at 650 to 750°C.

Fig. 3-16 Arrhenius plots of J_{RA} and J_{RP} for the NiSi(310Å)/p⁺n junctions fabricated with BF₂⁺ implantation at 35 keV to a dose of $5 \times 10^{15} \text{ cm}^{-2}$ followed by RTA at 750°C.

Fig. 3-17 Measured contact resistance vs. contact area for the NiSi/p⁺n contact formed by ITS scheme with BF₂⁺ implantation at 20keV to a dose of $5 \times 10^{15} \text{ cm}^{-2}$ followed by RTA at various temperatures.

Fig. 3-18 Measured contact resistivity for the NiSi/p⁺n contact formed by ITS scheme with BF₂⁺ implantation at 20keV to a dose of $5 \times 10^{15} \text{ cm}^{-2}$ followed by RTA at various temperatures. Data of four different contact areas are illustrated.

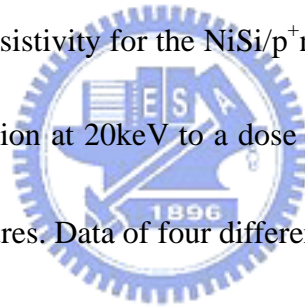


Fig. 3-19 Measured contact resistivity for the NiSi/p⁺n contact formed by ITS scheme with BF₂⁺ implantation at 35keV to a dose of $5 \times 10^{15} \text{ cm}^{-2}$ followed by RTA at various temperatures. Data of four different contact areas are illustrated.

Chapter 4

Fig. 4-1 The as-implanted phosphorus and fluorine profiles obtained by TRIM simulation for various P⁺ and F⁺ implantations.

Fig. 4-2 Forward ideality factor vs. annealing temperature for the NiSi(615Å)/n⁺p

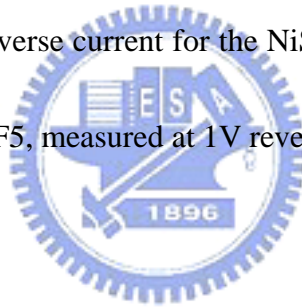
junction diodes.

Fig. 4-3 Reverse bias (5V) current density vs. annealing temperature for the NiSi(615Å)/n⁺p junction diodes with a junction area of 580×580μm².

Fig. 4-4 Area and peripheral leakage current densities for the NiSi(615Å)/n⁺p junction of sample P1F5 thermally annealed at 600 to 750°C.

Fig. 4-5 Typical I-V characteristic for the NiSi(615Å)/n⁺p junction of sample P1F5 fabricated with P⁺/F⁺ dual implantation at 35/30keV to a dose of 5×10¹⁵/5×10¹⁵cm⁻² followed by a 90 min thermal annealing at 750°C.

Fig. 4-6 Arrhenius plots of reverse current for the NiSi(615Å)/n⁺p junction of 750°C-annealed sample P1F5, measured at 1V reverse bias



Chapter 5

Fig. 5-1 Statistical distributions of reverse bias leakage current density for TaN/NiSi/p⁺n and TaN/Cu/NiSi/p⁺n junction diodes annealed at various temperatures.

Fig. 5-2 Sheet resistance vs. annealing temperature for TaN/NiSi/p⁺n and TaN/Cu/NiSi/p⁺n samples.

Fig. 5-3 SEM images showing top view (surface morphology) of TaN/Cu/NiSi/p⁺n sample annealed at (a) 350°C, (b) 425°C, (c) 475°C, and (d) 500°C.

Fig. 5-4 SEM images showing cross-sectional view of TaN/Cu/NiSi/p⁺n sample annealed at (a) 425°C, (b) 475°C, and (c) 500°C.

Fig. 5-5 XRD spectra of TaN/Cu/NiSi/p⁺n sample annealed at various temperatures.

Fig. 5-6 SIMS depth profiles of TaN/Cu/NiSi/p⁺n sample (a) as-fabricated and annealed at (b) 375°C, (c) 400°C, and (d) 500°C.

